Orbital precession ans shrinkage from frame rotation

M. W. Evans*, H. Eckardt†
Civil List, A.I.A.S. and UPITEC

(www.webarchive.org.uk, www.aias.us,
www.atomicprecision.com, www.upitec.org)

3 Numerical analysis and computation

3.1 Change of radius

According to Eq. (45), the change of radius dr/dt can be expressed by

$$\frac{dr}{dt} = -\frac{r\left(\left(\frac{d^2}{dt^2}\omega_1\right)t + 2\frac{d}{dt}\omega_1 + \frac{d}{dt}\omega\right)}{2\left(\left(\frac{d}{dt}\omega_1\right)t + \omega_1 + \omega\right)}. \tag{71}$$

For a graphical representation, the angular velocity ω has been approximated by the classical value

$$\omega = \frac{L}{mr^2} \tag{72}$$

with a constant angular momentum L. The radius function has been set to the elliptic orbit

$$r = \frac{\alpha}{1 + \epsilon\cos(\phi + \omega_1 t)}. \tag{73}$$

Thus the term $d\omega/dt$ in Eq. (71) can be computed directly from (73), giving a quite complicated expression. This can be evaluated for several model frame rotation speeds ω_1 as listed in Table 1.

The results are graphed in Figs. 1-4. Since r depends on the angle ϕ, we have plotted two curves for the extrema of r, appearing at angles 0 and π. For a decaying exponential function (Fig. 1) this gives an increase in orbital radius. An exponentially growing ω_1 leads to a radial shrinking (Fig. 2) with a phase shift for both angular positions. A hyperbolic function gives a radial increase again (Fig. 3), while a simple linear function leads to shrinking orbits in a wide range of time (Fig. 4).

*email: emyrone@aol.com
†email: mail@horst-eckardt.de

No.	ω_1
1	$\omega_0 \exp(-at)$
2	$\omega_0 \exp(at)$
3	$a/(t+c)$
4	$a\,t$

Table 1: Models of frame rotation for evaluating Eq. (71).

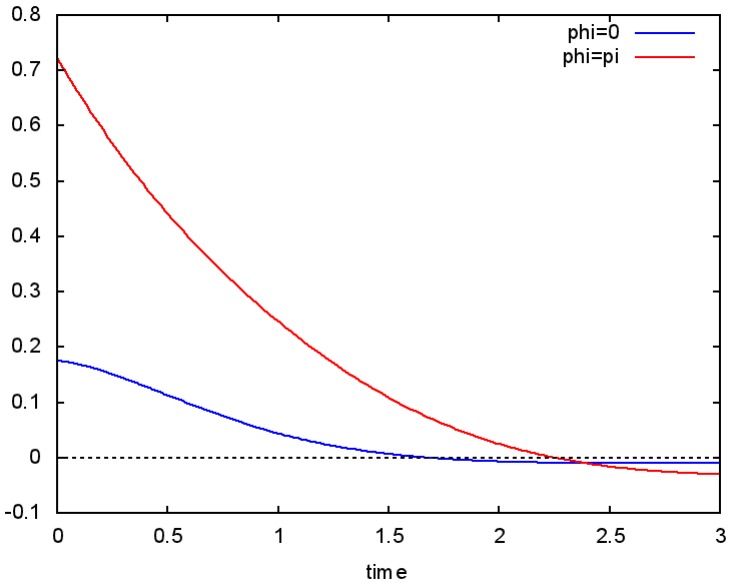

Figure 1: Function dr/dt for model 1 auf Table 1.

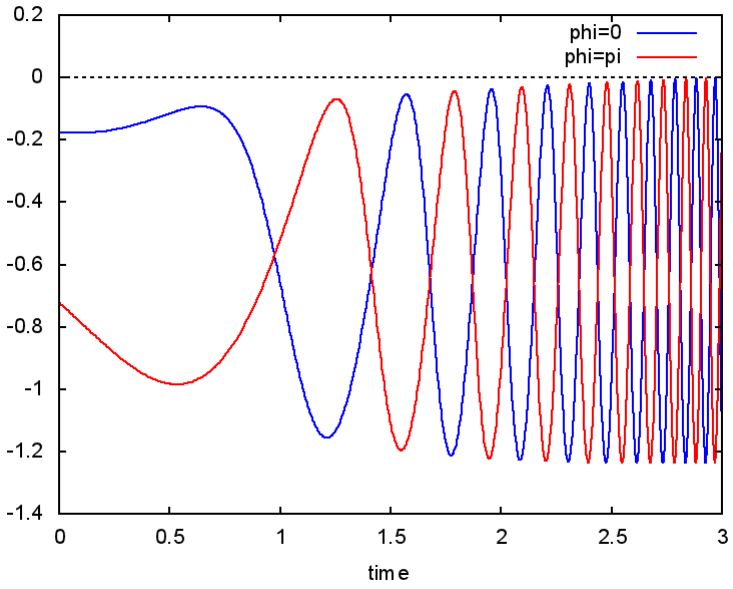

Figure 2: Function dr/dt for model 2 auf Table 1.

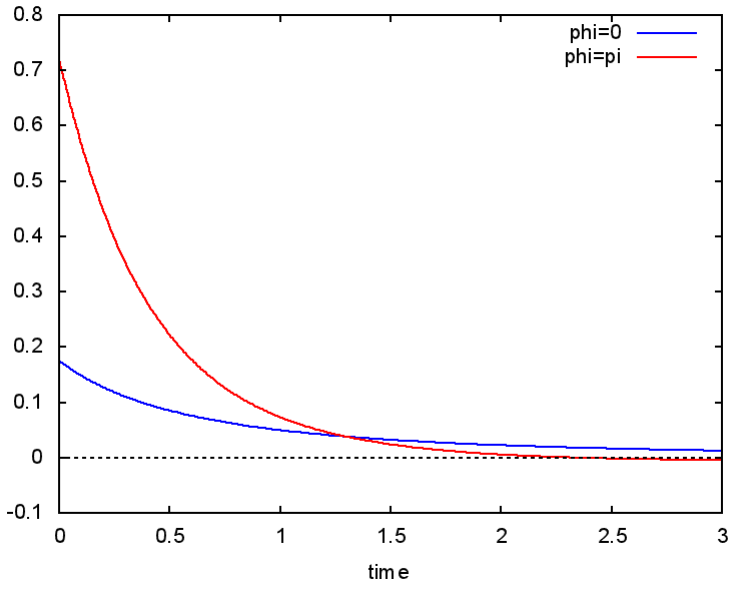

Figure 3: Function dr/dt for model 3 auf Table 1.

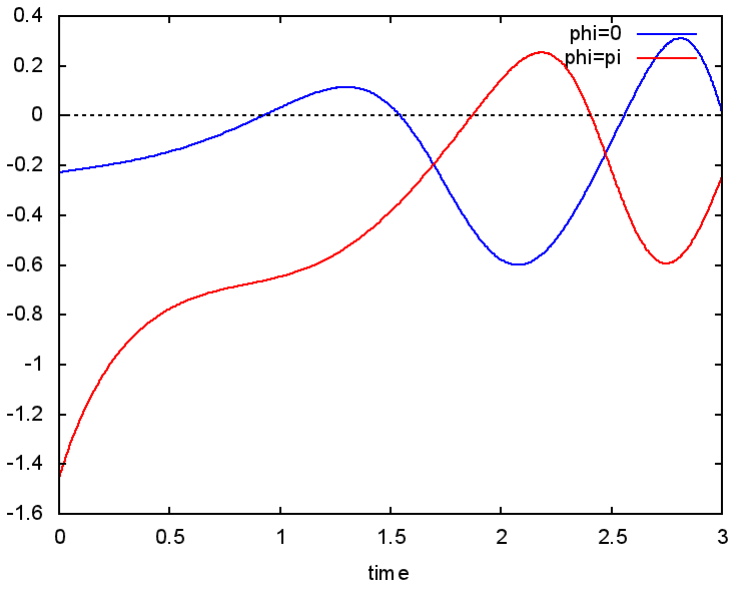

Figure 4: Function dr/dt for model 4 auf Table 1.

3.2 Numerical solution of Lagrange equations

The equations of motion (39,40) have been solved numerically for the canonical variables (r, ϕ) where ϕ is obtained from the frame rotation

$$\phi' = \phi + \omega_1 t. \tag{74}$$

These are the Lagrange equations obtained from the kinetic energy

$$T = \frac{m\left(r^2\left(\left(\frac{d}{dt}\omega_1\right)t + \frac{d}{dt}\phi + \omega_1\right)^2 + \left(\frac{d}{dt}r\right)^2\right)}{2} \tag{75}$$

and the potential energy

$$U = -\frac{mMG}{r} \tag{76}$$

with variables described in section 2. We used two models for the frame rotation, in the first case

$$\omega_1 = -a\exp(-b\,t). \tag{77}$$

with positive parameters a and b. All parameters within the calculation were chosen for a model system so that significant frame rotation effects appear. The orbit shows significant precession (Fig. 5). The constant of motion is the angular momentum

$$L = mr^2\dot{\phi}' = mr^2(\dot{\phi} + \omega_1 + \dot{\omega_1}\,t). \tag{78}$$

In Fig. 6 This angular momentum constant (L) is graphed together with the Newtonian angular momentum

$$L(\text{Newton}) = mr^2\dot{\phi}. \tag{79}$$

It can be seen that L is a constant of motion while L(Newton) is not.

The radialspin connection Ω_r was derived in Eq. (57). Since this form requires knowledge about the value of L which is not an input parameter of the calculation, we use the alternative form

$$\Omega_r = -\frac{r^2}{MG}\left(\dot{\omega_1}t + \omega_1\right)\left(\dot{\omega_1}t + 2\dot{\phi} + \omega_1\right). \tag{80}$$

as derived in note 413(5). Its graph is presented in Fig. 6 and shows oscillations stemming from the angular velocity $\omega = \dot{\phi}$. There is no shrinking in orbital radius or orbit period.

The second model for the frame rotation is a simple linearly increasing function

$$\omega_1 = a\,t. \tag{81}$$

Since ω_1 is opposed to the direction of the orbiting mass on the ellipse, there is a value of t where ω_1 exceeds the angular velocity ω of the mass. Consequently, the direction of motion reverses, leading to very exotic orbits as presented in Fig. 8. Nonetheless, the constant of motion L is preserved as can be seen from

Fig. 9. Due to the exotic orbit, the Newtonian angular momentum oscillates strongly and changes direction multiply (see zero crossings). Similarly, the spin connection Ω_r (Fig. 10) oscillates strongly in the negative range. From other models of ω_1 we found that Ω_r can also take positive values.

In this second model, ω_1 grows beyond all limits so that we would expect a drastic shrinking of orbit. The observed maximum radii and periods per single orbit were extracted from the calculation, interpolated to increase precision, and compiled in Table 2. It can be seen that both quantities are constant within calculational precision of 4-5 digits. The explanation is found when considering the single angular terms of the constant of motion (78), see Fig. 11. The terms ω_1 and $\dot{\omega_1}t$ (red/green line) are positive and identical according to Eq. (81). After the first oscillation, both terms exceed the bottom part of ω (purple line). As a consequence, ω sinks below zero so that the sum of all three terms gives the same sum curve (blue line) all over the time. The blue line corresponds to $1/r^2$ so that L remains constant. Since the blue curve does not change from oscillation to oscillation, there is no change in orbital radius. The reversal of angular motion is a consequence of keeping L constant.

In total, the dynamics of the system works in a way that orbital parameters $r_{\max}$ and ΔT are conserved. In other words, frame rotation leads to strong precession and even reversing of orbital motion, but the basic parameters of the orbit are maintained.

$r_{\max}$	ΔT
3.175345	5.993880
3.175353	5.993257
3.175360	5.993402
3.175367	5.993437
3.175374	5.993444
3.175381	5.993456
3.175388	5.993469
3.175394	5.993483
3.175402	5.993503

Table 2: Maximum orbital radii and orbit periods of model (81).

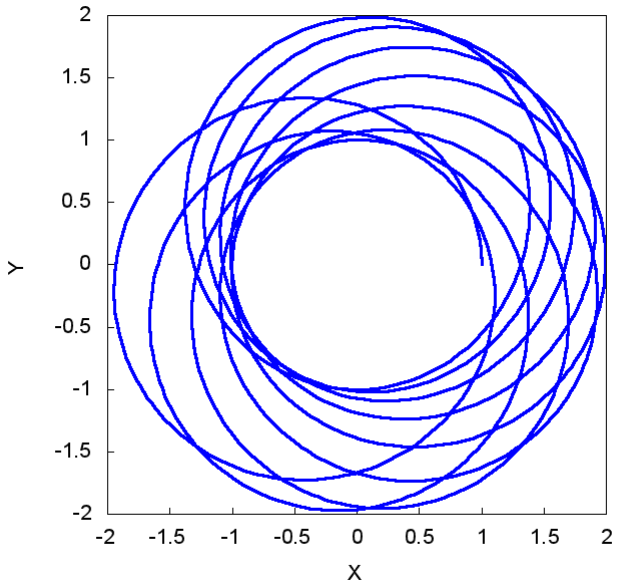

Figure 5: Precessing orbit of model (77).

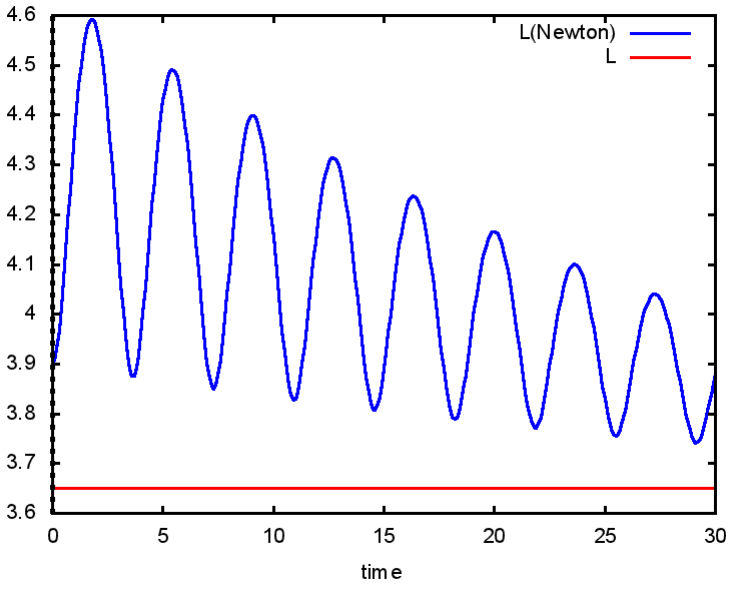

Figure 6: Angular momenta of model (77).

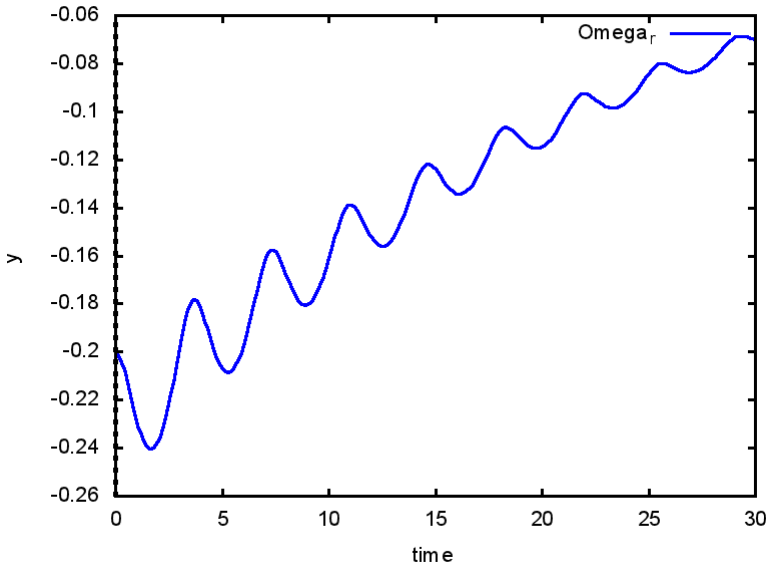

Figure 7: Spin connection Ω_r of model (77).

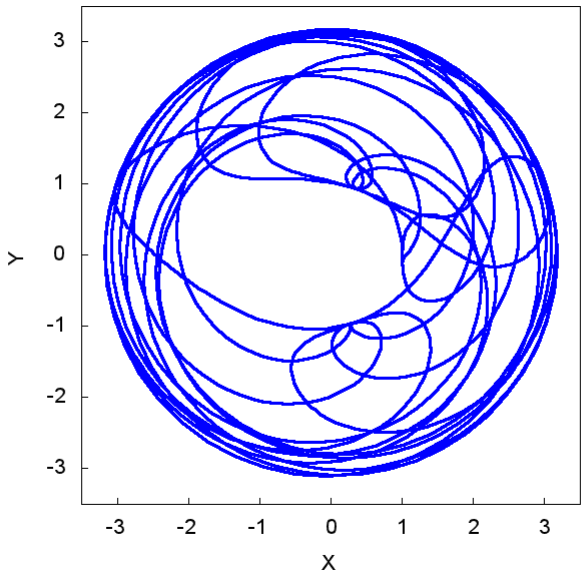

Figure 8: Precessing orbit of model (81).

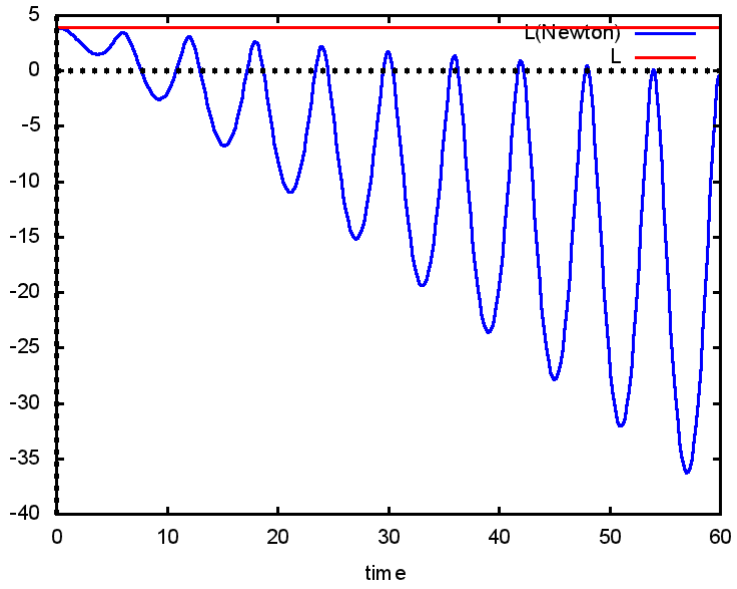

Figure 9: Angular momenta of model (81).

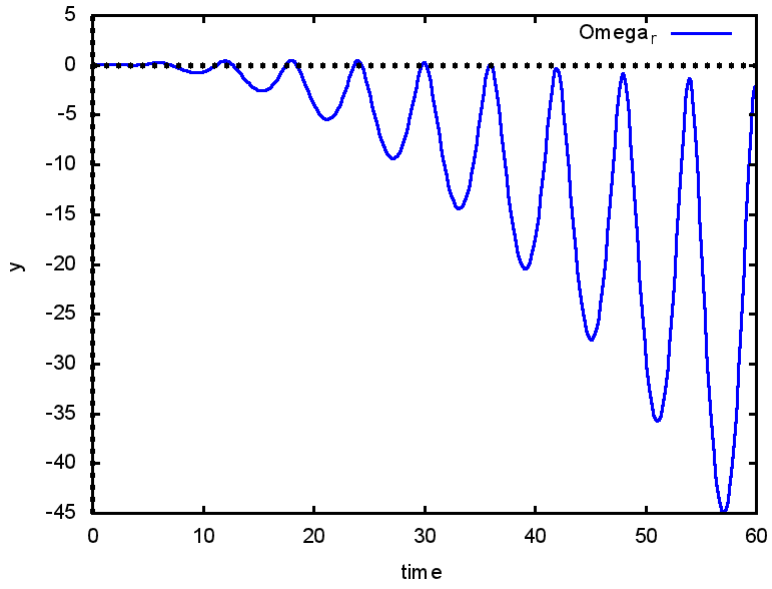

Figure 10: Spin connection Ω_r of model (81).

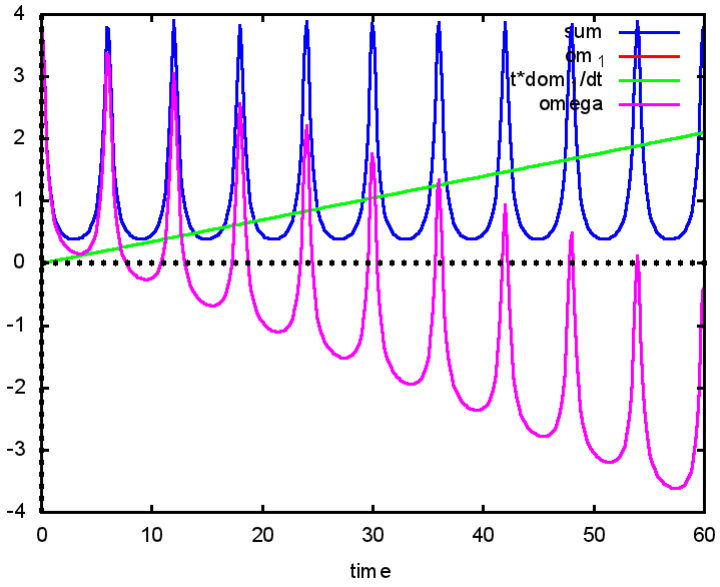

Figure 11: Single terms of constant of motion (81).